# Convex Optimization of Thin Airfoils Using Cubic Splines

Daniel C. Berkenstock * and Juan J. Alonso†
*Stanford University, Stanford, CA 94305, USA*

Laurent Lessard‡
*Northeastern University, Boston, MA, 02115, USA*

**Convex optimization offers an attractive approach to the physical design of aerospace vehicles due to its ability to quickly identify global optima to relatively complex problems. Building on previous work, we show a significant improvement in optimal supersonic drag coefficient for airfoils parameterized by cubic splines, versus cubic polynomials. In particular we derive convex expressions for the supersonic lift and drag coefficients of thin airfoils expressed as cubic splines, as well as subsonic lift and moment coefficients for the same. We compare the results of globally optimal designs parameterized by cubic polynomials and cubic splines, showing improvements in drag performance of approximately 20-30%. These designs are computed typically in single digit seconds using commodity hardware and open source software tools.**

## I. Introduction

In this paper, we extend our prior work[1] on the convex optimization of thin airfoils using cubic polynomials to include airfoils defined by cubic splines. We refer the reader to our previous paper for a general primer on convex optimization and its applicability to Aerodynamic Shape Optimization (ASO) as well as background references.

As before, we explore the benefits and limitations of casting conceptual airfoil design as a convex optimization problem. Recall that a convex optimization problem takes the general form

$$\begin{aligned} \underset{x}{\text{minimize}} \quad & f_0(x) \\ \text{subject to} \quad & f_i(x) \leq 0, \ i = 1, \ldots, m, \end{aligned} \tag{1}$$

where $x \in \mathbb{R}^n$ is a vector of design variables and the $f_i : \mathbb{R}^n \to \mathbb{R}$ are convex objective and constraint functions. A function $f : \mathbb{R}^n \to \mathbb{R}$ is convex if the domain of $f$ ($\text{dom} f$) is a convex set and if for all $x, y \in \text{dom} f$, with $0 \leq \theta \leq 1$,

$$f(\theta x + (1-\theta)y) \leq \theta f(x) + (1-\theta) f(y). \tag{2}$$

From a geometric point of view, this describes a function that lies below the line segment connecting any two points of its graph. For a comprehensive discussion of convex optimization and convex functions we refer the reader to the book by Boyd and Vandenberghe [2]. A list of common convex functions and their domains is included in Table 1.

Splines have been used extensively in the design of airfoils and other aerodynamic shapes. For example, Song and Keane[3], Masters et al.[4], and Sripawadkul, Padulo, and Guenov[5] all provide excellent overviews of shape paramerization techniques for aerospace shape optimization, including the use of splines. The well-known Class-Shape-Transformation (CST) method [6–8] for shape parameterization employs Bernstein polynomials. In [9], Rajnarayan et al describe a universal shape parameterization for airfoils using B-splines. Also, in [10], Li and Krist discuss the benefits of incorporating curvature-based smoothing techniques in the optimization of transonic airfoils. In general, the use of various types of splines, including surface and volumetric, has been well studied in the design of airfoils and more general aerodynamic shapes.

In this paper, we make several contributions. First, we derive closed-form solutions for lift, drag, and moment coefficients using thin-airfoil theory, across several flow regimes, for the case of airfoils defined by cubic splines. We also show that important performance indicators, under these assumptions, are convex functions. Finally, we present case studies that illustrate the benefits of a cubic spline approach and compare results versus the cubic polynomial case. Through these case studies, we also assess the impact of important parameters such as number of spline segments and curvature regularization for fair surface design.

*PhD Candidate, Department of Aeronautics and Astronautics.
†Vance D. and Arlene C. Coffman Professor, Department of Aeronautics and Astronautics, AIAA Fellow.
‡Associate Professor, Mechanical and Industrial Engineering.

| Function | Definition | Domain | Curvature |
|---|---|---|---|
| Summation | $\sum_{ij} X_{ij}$ | $X \in \mathbb{R}^{m\times n}$ | convex |
| Max | $\max_{ij}\{X_{ij}\}$ | $X \in \mathbb{R}^{m\times n}$ | convex |
| Min | $\min_{ij}\{X_{ij}\}$ | $X \in \mathbb{R}^{m\times n}$ | concave |
| 2-norm | $\sqrt{\sum_i x_i^2}$ | $x \in \mathbb{R}^n$ | convex |
| Positive semidefinite quadratic form | $x^T P x$ | $x \in \mathbb{R}^n$, $P \succeq 0$ | convex |
| Quadratic over linear | $x^T x/y$ | $x \in \mathbb{R}^n$, $y > 0$ | convex |
| Inverse positive | $1/x$ | $x > 0$ | convex |

**Table 1 Representative convex functions**

## II. Application of Thin-Airfoil Theory to Cubic Spline Airfoils

In this work, we consider *cubic spline airfoils*, which are airfoils defined by separate cubic splines representing the upper and lower surfaces. These splines are defined by a series of cubic polynomials, which are constrained to have $C^2$ continuity across the airfoil surface[11]. The polynomials are each defined over a subset of the knot vector, $x_k = [x_{k_0}, x_{k_1}, \ldots, x_{k_n}]$. Our approach is general and can be used with explicit polynomials of arbitrary degree. In other words, our current method is restricted for polynomials for which $y = f(x)$. However, for simplicity and ease of exposition, we will restrict ourselves to cubic polynomials for the remainder of the paper, so that, for the span, $x \in [x_{k_i}, x_{k_{i+1}}]$,

$$y_u(x) = a_{u_i}x^3 + b_{u_i}x^2 + c_{u_i}x + d_{u_i} \qquad \text{and} \qquad y_l(x) = a_{l_i}x^3 + b_{l_i}x^2 + c_{l_i}x + d_{l_i} \tag{3}$$

where, in order to ensure a closed shape, both surfaces must meet at the leading and trailing edges of the airfoil, separated by the aerodynamic chord, which without loss of generality we assume to have length equal to unity, so that,

$$y_{u_0}(0) = y_{l_0}(0) = 0 \qquad \text{and} \qquad y_{u_n}(1) = y_{l_n}(1) = 0. \tag{4}$$

Furthermore, in order to enforce $C^2$ continuity, we enforce the following constraints at each point in the knot vector,

$$y_{u_i}(x_{k_{i+1}}) = y_{u_{i+1}}(x_{k_{i+1}}) \qquad \text{and} \qquad y_{l_i}(x_{k_{i+1}}) = y_{l_{i+1}}(x_{k_{i+1}}), \tag{5}$$

and also,

$$y'_{u_i}(x_{k_{i+1}}) = y'_{u_{i+1}}(x_{k_{i+1}}) \qquad \text{and} \qquad y'_{l_i}(x_{k_{i+1}}) = y'_{l_{i+1}}(x_{k_{i+1}}), \tag{6}$$

and,

$$y''_{u_i}(x_{k_{i+1}}) = y''_{u_{i+1}}(x_{k_{i+1}}) \qquad \text{and} \qquad y''_{l_i}(x_{k_{i+1}}) = y''_{l_{i+1}}(x_{k_{i+1}}). \tag{7}$$

We now proceed to analyze the aerodynamic properties of cubic spline airfoils in subsonic and supersonic flows. In each circumstance we will employ thin-airfoil theory, under which we assume the thickness and camber of the airfoil is small compared to the chord. In addition, we also implicitly assume that the leading-edge radius of the airfoil is small. In fact, as we focus on supersonic aerodynamic performance we allow for sharp leading edges.

### A. Thin Airfoil Aerodynamics: Subsonic Cubic Spline Airfoils

Thin-airfoil theory provides closed form analytic solutions for the lift and moment coefficients of a reasonably thin airfoil in a subsonic, invsicid, irrotational, incompressible flow. As presented in [12], the sectional lift and moment coefficients are dependent solely upon the shape of the camber line,

$$z_i(x) = \frac{y_{u_i}(x) + y_{l_i}(x)}{2} = \frac{(a_{u_i} + a_{l_i})x^3 + (b_{u_i} + b_{l_i})x^2 + (c_{u_i} + c_{l_i})x + (d_{u_i} + d_{l_i})}{2}, \tag{8}$$

for $x \in [x_{k_i}, x_{k_{i+1}}]$, and its slope

$$\frac{\mathrm{d}z_i}{\mathrm{d}x} = \frac{3(a_{u_i} + a_{l_i})x^2 + 2(b_{u_i} + b_{l_i})x + (c_{u_i} + c_{l_i})}{2}. \tag{9}$$

For simplicity of integration, we employ the conventional cosine transformation $x = \frac{1}{2}(1 - \cos\theta)$, so that, once simplified,

$$\frac{\mathrm{d}z_i}{\mathrm{d}x} = \frac{1}{2}\left(3(a_{u_i} + a_{l_i})\cos^4\frac{\theta}{2} + (b_{u_i} + b_{l_i})(1 + \cos\theta) + c_{u_i} + c_{l_i}\right). \tag{10}$$

The sectional lift coefficient is $c_l = 2\pi(\alpha - \alpha_{l0})$, where the angle of zero lift is given by

$$\alpha_{l0} = \frac{1}{\pi}\int_0^\pi \frac{\mathrm{d}z}{\mathrm{d}x}(1 - \cos\theta)\,\mathrm{d}\theta = \frac{1}{\pi}\sum_i \int_{\theta_i}^{\theta_{i+1}} \frac{\mathrm{d}z_i}{\mathrm{d}x}(1 - \cos\theta)\,\mathrm{d}\theta, \tag{11}$$

where $\theta_i = \arccos(1 - 2x_i)$. Similarly, the moment coefficient about the aerodynamic center is

$$c_{\mathrm{mac}} = -\frac{1}{2}\int_0^\pi \frac{\mathrm{d}z}{\mathrm{d}x}(\cos\theta - \cos 2\theta)\,\mathrm{d}\theta = -\frac{1}{2}\sum_i \int_{\theta_i}^{\theta_{i+1}} \frac{\mathrm{d}z_i}{\mathrm{d}x}(\cos\theta - \cos 2\theta)\,\mathrm{d}\theta. \tag{12}$$

Evaluating the above integrals, we obtain

$$\begin{aligned} 32\pi\alpha_{l0} = \sum_{i=0}^{n-1} \Big[ & 2(\theta_{i+1} - \theta_i)\left(3(a_{u_i} + a_{l_i}) + 4(b_{u_i} + b_{l_i}) + 8(c_{u_i} + c_{l_i})\right) \\ & + (\sin\theta_{i+1} - \sin\theta_i)(3(a_{u_i} + a_{l_i}) + 16(c_{u_i} + c_{l_i})) \\ & (\sin(2\theta_i) - \sin(2\theta_{i+1}))(3(a_{u_i} + a_{l_i}) + 4(b_{u_i} + b_{l_i})) \\ & (\sin(3\theta_i) - \sin(3\theta_{i+1}))(a_{u_i} + a_{l_i})\Big], \end{aligned} \tag{13}$$

and

$$\begin{aligned} 768c_{\mathrm{mac}} = \sum_{i=0}^{n-1} \Big[ & 12(\theta_i - \theta_{i+1} + \sin\theta_i - \sin\theta_{i+1})(9(a_{u_i} + a_{l_i}) + 8(b_{u_i} + b_{l_i})) \\ & + 12(\sin(2\theta_{i+1}) - \sin(2\theta_i))(3(a_{u_i} + a_{l_i}) + 4(b_{u_i} + b_{l_i}) + 8(c_{u_i} + c_{l_i})) \\ & + 4(\sin(3\theta_{i+1}) - \sin(3\theta_i))(9(a_{u_i} + a_{l_i}) + 8(b_{u_i} + b_{l_i})) \\ & + 9(\sin(4\theta_{i+1}) - \sin(4\theta_i))(a_{u_i} + a_{l_i})\Big]. \end{aligned} \tag{14}$$

For the subsonic case, and under thin airfoil assumptions, $c_l$, $c_{\mathrm{mac}}$, and $\alpha_{l0}$ are affine, and therefore convex, functions of the upper and lower surface spline coefficients and the angle of attack $\alpha$.

### B. Thin Airfoil Aerodynamics: Supersonic Cubic Spline Airfoils

As detailed in Kuethe and Chow[13], under suitable assumptions (including small thickness, camber, and angle of attack and sharp leading edges), the lift and drag coefficients of an airfoil in a supersonic flow may be approximated as

$$c_l = \frac{4\alpha}{\sqrt{M^2 - 1}} \qquad \text{and} \qquad c_d = \frac{4}{\sqrt{M^2 - 1}}\left(\alpha^2 + K_2 + K_3\right). \tag{15}$$

Here we will again assume a chord length of 1. The $K_2$ term accounts for wave drag created by the camber line,

$$K_2 = \int_0^1 \left[\frac{\mathrm{d}}{\mathrm{d}x}\left(\frac{y_u(x) + y_l(x)}{2}\right)\right]^2 \mathrm{d}x, \tag{16}$$

and the $K_3$ term accounts for wave drag generated by the airfoil thickness,

$$K_3 = \int_0^1 \left[\frac{\mathrm{d}}{\mathrm{d}x}\left(\frac{y_u(x) - y_l(x)}{2}\right)\right]^2 \mathrm{d}x. \tag{17}$$

Following a similar approach as the previous section, we find that, for the cubic spline case, the drag coefficient may be represented as a sum of quadratic forms in the spline coefficients and the angle of attack. Specifically,

$c_d = \frac{4}{\sqrt{M^2-1}} \sum_i v_i^T Q_i v_i$, where

$$Q_i = \frac{1}{2}\begin{bmatrix} 2/n & 0 & 0 & 0 & 0 & 0 & 0 \\ 0 & \frac{9}{5}(x_{k_{i+1}}^5 - x_{k_i}^5) & \frac{3}{2}(x_{k_{i+1}}^4 - x_{k_i}^4) & (x_{k_{i+1}}^3 - x_{k_i}^3) & 0 & 0 & 0 \\ 0 & \frac{3}{2}(x_{k_{i+1}}^4 - x_{k_i}^4) & \frac{4}{3}(x_{k_{i+1}}^3 - x_{k_i}^3) & (x_{k_{i+1}}^2 - x_{k_i}^2) & 0 & 0 & 0 \\ 0 & (x_{k_{i+1}}^3 - x_{k_i}^3) & (x_{k_{i+1}}^2 - x_{k_i}^2) & (x_{k_{i+1}} - x_{k_i}) & 0 & 0 & 0 \\ 0 & 0 & 0 & 0 & \frac{9}{5}(x_{k_{i+1}}^5 - x_{k_i}^5) & \frac{3}{2}(x_{k_{i+1}}^4 - x_{k_i}^4) & (x_{k_{i+1}}^3 - x_{k_i}^3) \\ 0 & 0 & 0 & 0 & \frac{3}{2}(x_{k_{i+1}}^4 - x_{k_i}^4) & \frac{4}{3}(x_{k_{i+1}}^3 - x_{k_i}^3) & (x_{k_{i+1}}^2 - x_{k_i}^2) \\ 0 & 0 & 0 & 0 & (x_{k_{i+1}}^3 - x_{k_i}^3) & (x_{k_{i+1}}^2 - x_{k_i}^2) & (x_{k_{i+1}} - x_{k_i}) \end{bmatrix}, \tag{18}$$

and

$$v_i^T = \begin{bmatrix} \alpha & a_{u_i} & b_{u_i} & c_{u_i} & d_{u_i} & a_{l_i} & b_{l_i} & c_{l_i} & d_{l_i} \end{bmatrix}. \tag{19}$$

It is straightforward to check that all eigenvalues of $Q_i$ are positive, and so $Q_i$ is positive definite, and $c_d$ is a convex function of $v$, as a summation of a set of convex quadratic forms.

Given that the lift coefficient is represented by a linear function in supersonic thin-airfoil theory, the drag-to-lift ratio is the ratio of a quadratic to a linear function,

$$\frac{D}{L} = \frac{\sum_i v_i^T Q_i v_i}{\alpha}. \tag{20}$$

Per the above analysis, this is, in fact, the ratio of a *positive definite* quadratic over a linear function. Therefore, imposing an upper bound on $D/L$ (or equivalently, a lower bound on $L/D$) over the set $\{\alpha > 0\}$ is convex-representable.

## III. Geometric Constraints

A number of useful geometric constraints may be modeled as constraints that are convex in the spline parameters of the airfoil. In some cases, these are individual constraints, whereas in others they are multiple constraints, sampled uniformly over the chord of the airfoil. A number of these constraints are described below.

### A. Single Constraints

As a linear function of the spline coefficients, constraints on both minimum and maximum area are convex. Additionally, arc length may be approximated as a sum of 2-norms, a convex function, indicating that specifying a maximum arc length is also a convex constraint. These are both examples of constraints which are integrated over the complete airfoil section and are further detailed below.

*1. Minimum or Maximum Area*

The enclosed area of an airfoil represents the amount of payload that could be contained within, especially in the case that payload is a liquid, such as fuel. The area is calculated as the integral of the thickness of the airfoil between the leading and trailing edges,

$$\begin{aligned} A &= \int_0^1 (y_u(x) - y_l(x))\,\mathrm{d}x \\ &= \sum_i (a_{u_i} - a_{l_i})(x_{k_{i+1}}^4 - x_{k_i}^4) + (b_{u_i} - b_{l_i})(x_{k_{i+1}}^3 - x_{k_i}^3) + (c_{u_i} - c_{l_i})(x_{k_{i+1}}^2 - x_{k_i}^2) + (d_{u_i} - d_{l_i})(x_{k_{i+1}} - x_{k_i}). \end{aligned} \tag{21}$$

*2. Maximum Arc Length*

The arc length of a cubic spline does not have a readily available closed form solution, as

$$l = \int_0^1 \sqrt{1 + \left(\frac{\mathrm{d}y}{\mathrm{d}x}\right)^2}\,\mathrm{d}x \tag{22}$$

results in an elliptic integral. However, it may be approximated to arbitrary precision as a summation of norms, resulting in the convex constraints,

$$\sum_i \left\| \begin{bmatrix} y_u(x_{i+1}) - y_u(x_i) \\ x_{i+1} - x_i \end{bmatrix} \right\| \le l_{u_{\max}} \qquad \text{and} \qquad \sum_i \left\| \begin{bmatrix} y_l(x_{i+1}) - y_l(x_i) \\ x_{i+1} - x_i \end{bmatrix} \right\| \le l_{l_{\max}}. \tag{23}$$

**B. Sampled Constraints**

The constraints described in this section reflect properties across a range of $x$ values. For example, if we are interested in some property $g(x, v)$ that depends on the position $x$ along the chord and the airfoil parameters $v$ (e.g., the spline coefficients $a_i$, $b_i$, $c_i$, and $d_i$), constraints that bound the maximum or minimum over some subset $x \in S$ of possible $x$ values would take the form

$$\max_{x \in S} g(x, v) \le g_{\max} \qquad \text{or} \qquad \min_{x \in S} g(x, v) \ge g_{\min}. \tag{24}$$

These constraints are convex in $v$ provided $g$ is a convex function of $v$ (for the $g_{\max}$ constraint) or $g$ is a concave function of $v$ (for the $g_{\min}$ constraint). Indeed, (24) can be rewritten as

$$g(x, v) \le g_{\max} \quad \text{for all } x \in S, \qquad \text{or} \qquad g(x, v) \ge g_{\min} \quad \text{for all } x \in S. \tag{25}$$

When $g$ is an affine function of $v$, both constraints are convex. However, these constraints can be difficult to incorporate into a numerical solver because when $S$ contains infinitely many points, such as within an interval $S = [x_1, x_2]$, the constraints (25) correspond to infinitely many constraints (one for each $x \in S$). This limitation can be overcome by *sampling*. In other words, we pick a finite set of representative points $\{x_1, x_2, \ldots, x_m\} \subset S$ and instead impose the constraints

$$g(x_k, v) \le g_{\max} \quad \text{for } k = 1, \ldots, m, \qquad \text{or} \qquad g(x_k, v) \ge g_{\min} \quad \text{for } k = 1, \ldots, m. \tag{26}$$

Below we describe some examples of constraints that can be modeled in this fashion and their associated $g$ functions.

*1. Thickness*

Often it is desirable to place minimum or maximum limits on the thickness, $\tau = y_u - y_l$, of an airfoil. These constraints may be specified over the entire airfoil, or a region, $x \in [x_1, x_2]$, and the corresponding $g$ function is

$$g(x) = y_u(x) - y_l(x). \tag{27}$$

This function is affine in the airfoil parameters, so we can impose either upper or lower bound constraints. In order to prevent unwanted intersections between the upper and lower surfaces, we generally include the constraint $g(x) \ge 0$ for $x \in [0, 1]$.

*2. Gradient and Curvature Constraints*

It may be desirable to place limitations on the derivatives of the shape, for instance in order to prevent large pressure gradients that may lead to flow separation. This may be done for curvature using the $g$ function

$$g(x) = 6a_{u_i}x + 2b_{u_i}, \tag{28}$$

or for the gradient (first derivative, more relevant in supersonic flow) using the $g$ function

$$g(x) = 3a_{u_i}x^2 + 2b_{u_i}x + c_{u_i}. \tag{29}$$

These functions are affine in the airfoil spline coefficients, so it is possible to impose upper or lower bound constraints on either one.

*3. Internal Payloads*

Beyond the constraints discussed above, it may be important to fit various shapes into the internal cavity of the airfoil. For instance, a circle of radius, $r$, centered at $[x_c, y_c]$, can be prescribed by including the following sampled constraints, which correspond to the upper and lower surfaces, respectively:

$$g(\theta) = \begin{cases} a_{u_i}(x_c + r\cos\theta)^3 + b_{u_i}(x_c + r\cos\theta)^2 + c_{u_i}(x_c + r\cos\theta) + d_{u_i} - y_c - r\sin\theta) \geq 0 & \text{for all } \theta \in [0, \pi] \\ a_{l_i}(x_c + r\cos\theta)^3 + b_{l_i}(x_c + r\cos\theta)^2 + c_{l_i}(x_c + r\cos\theta) + d_{l_i} - y_c - r\sin\theta) \leq 0 & \text{for all } \theta \in [\pi, 2\pi]. \end{cases} \tag{30}$$

An internal square constraint may be defined as a minimum thickness constraint over a window centered at $x_c$ and $y_c$. For constant $x_c$, $y_c$, and $r$ these each describe affine constraints. In fact, since $y_c$ appears as a linear term it is also possible to include it as a convex variable. This is not true for $x_c$, the inclusion of which would result in several bilinear terms.

## IV. Application to Airfoil Design

In the previous sections, we provided an overview of several indicators of performance and a number of constraints that may be modeled as convex functions of the parameters of a given thin, cubic spline airfoil. To summarize the previous sections, Table 2 highlights a subset of objective functions and constraints that can be easily included in convex optimization problems for airfoil design based on thin-airfoil theory. The power of this approach lies in the ability to pick arbitrarily from this menu since any convex combination of convex functions is also convex.

| **Aerodynamic Performance** | **Geometric Constraints** |
|---|---|
| Subsonic lift coefficient | Minimum/Maximum thickness |
| Subsonic moment coefficient | Minimum/Maximum area |
| Supersonic drag coefficient | Minimum/Maximum gradient |
| Supersonic lift to drag ratio | Minimum/Maximum curvature |
| Supersonic moment coefficient | Internal payload constraints |
| | Non-Intersection constraint |
| | Maximum arc length constraint |

**Table 2 Design of thin, cubic spline airfoils: convex objectives and constraints**

In the remaining sections of this paper, we demonstrate applications of this approach using several examples of increasing complexity. First we demonstrate the approach via a simple area maximization problem. Next, we consider minimization of drag of a zero lift airfoil in a supersonic flow, a problem with a convex quadratic objective function and convex constraints. Then we explore the convergence of this method based on two key parameters, the number of spline segments used to define the airfoil shape and a regularization parameter used to control maximum curvature. Finally, similarly to the polynomial case in our previous work, we demonstrate the extension of this method to a single nonconvex variable using a golden search algorithm.

### A. Solving Convex Optimization Problems

Several readily available packages, including CVXPY [14, 15] and YALMIP [16], are modeling languages that efficiently and automatically transform a convex optimization problem into a standard form, call an external solver, and post-process the results. For example, CVXPY uses graph implementations of convex functions to transform the initial problem into a conic form, which is a generalization of a linear program. These conic problems are then readily solvable using a combination of commercial or open-source solvers.

As an example, consider the problem of maximizing the area between an upper surface and the x axis, with the maximum thickness constraints $y_u(x) \leq 0.5$ whenever $0 \leq x \leq 0.4$ and $y_u(x) \leq 1.0$ whenever $0.4 \leq x \leq 1.0$. This problem may be expressed as the optimization problem,

$$\text{area} = \sum_i \frac{a_{u_i}}{4}(x_{k_{i+1}}^4 - x_{k_i}^4) + \frac{b_{u_i}}{3}(x_{k_{i+1}}^3 - x_{k_i}^3) + \frac{c_{u_i}}{2}(x_{k_{i+1}}^2 - x_{k_i}^2) + d_{u_i}(x_{k_{i+1}} - x_{k_i}) \tag{31}$$

$$\begin{aligned}
\underset{\{a_{u_i}, b_{u_i}, c_{u_i}, d_{u_i}\}}{\text{minimize}} \quad & \frac{1}{\text{area}} + \epsilon \left\| a_u \right\|^2 && \text{(function describing the area)} \\
\text{subject to} \quad & \max_{x \in [0, 0.4]} a_{u_i} x^3 + b_{u_i} x^2 + c_{u_i} x + d_{u_i} \leq 0.5 && \text{(thickness constraint)} \\
& \max_{x \in [0.4, 1.0]} a_{u_i} x^3 + b_{u_i} x^2 + c_{u_i} x + d_{u_i} \leq 1.0 && \text{(thickness constraint)} \\
& \min_{x \in [0, 1]} a_{u_i} x^3 + b_{u_i} x^2 + c_{u_i} x + d_{u_i} \geq 0 && \text{(non-intersection constraint)}
\end{aligned} \tag{32}$$

Here, we include a small amount of regularization on the total curvature, which minimizes the effects of numerical rounding errors that are introduced in the purely linear approach. The solution, employing uniformly sampled maximum thickness and non-intersection constraints, is shown in Figure 1. For a uniformly sampled knot vector with $n = 5$ and $\epsilon = 1e - 4$, the maximum area is $\text{area}_{\text{max}} = 1.649$.

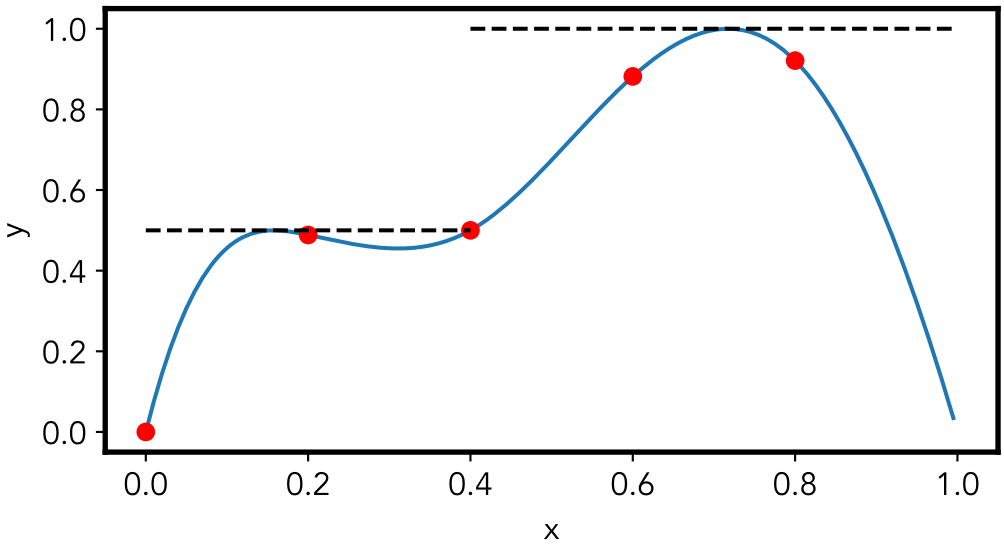


**Fig. 1 Maximum area cubic spline subject to partial thickness constraints (dashed lines denote constraints, red dots denote knot locations).**

### B. Minimum Drag Supersonic Airfoil Comparison: Cubic Polynomials vs Cubic Splines

Moving on to a more pertinent example, let us consider the case of drag minimization of a supersonic, non-lifting airfoil. Formally, we seek to minimize drag, subject to a non-intersection constraint and the constraint that the airfoil enclose a circular payload, centered at the location $x_c$, which is a given constant. We also impose a minimum subsonic lift at zero angle of attack and a maximum subsonic moment about the mean aerodynamic center. The vector of design variables for the quadratic form of drag with this problem is $v_i^T = \begin{bmatrix} \alpha & a_{u_i} & b_{u_i} & c_{u_i} & d_{u_i} & a_{l_i} & b_{l_i} & c_{l_i} & d_{l_i} \end{bmatrix}$, and

the problem may be formally stated as,

$$
\begin{aligned}
\underset{v,y_c}{\text{minimize}} \quad & \frac{4}{\sqrt{M^2-1}} \sum_i v_i^T Q_i v_i \\
\text{subject to} \quad & \alpha_{l0} \leq \alpha_{l0_{\min}} \\
& c_{\text{mac}} \leq c_{\text{mac}_{\max}} \\
& \alpha = 0 \\
& \min_{x\in[0,1]} \left(y_u(x) - y_l(x)\right) \geq 0 \\
& \max_{x\in[0,1]} |y_u''(x) - y_l''(x)| \leq \kappa_{\max} \\
& \min_{\theta\in[0,\pi]} \left(a_{u_i}(x_c + r\cos\theta)^3 + b_{u_i}(x_c + r\cos\theta)^2 + c_{u_i}(x_c + r\cos\theta) + d_{u_i} - y_c - r\sin\theta\right) \geq 0 \\
& \max_{\theta\in[\pi,2\pi]} \left(a_{l_i}(x_c + r\cos\theta)^3 + b_{l_i}(x_c + r\cos\theta)^2 + c_{l_i}(x_c + r\cos\theta) + d_{l_i} - y_c - r\sin\theta\right) \leq 0.
\end{aligned}
\tag{33}
$$

In this example, we specify $M = 2$, $\alpha_{l0_{\min}} = -0.15$, $c_{\text{mac}_{\max}} = -0.2$, $\kappa_{\max} = 5$, $x_c = 0.35$ and $r = 0.05$, with a constraint sampling interval $\Delta x = 0.001$. The ability to limit or penalize maximum curvature, or variation of curvature, becomes important in the case of a spline surface, as numerical solutions without any such limitations often result in physically undesirable, or wavy, surfaces. We will explore this further in the next section.

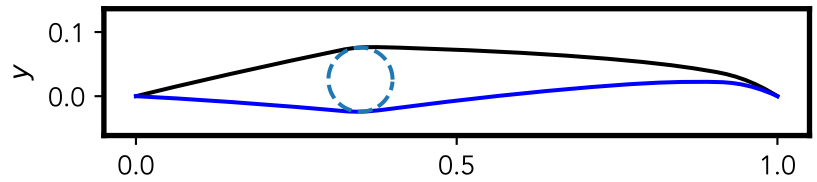


a) Optimal thin airfoil derived using cubic spline surfaces

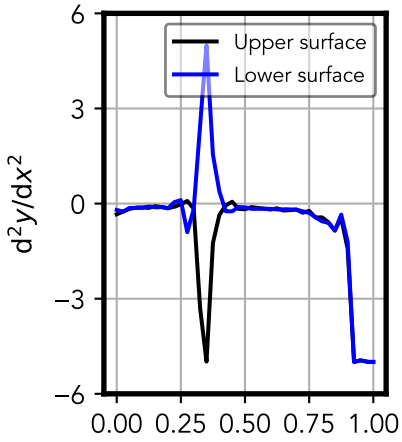


b) Curvature profile of optimal cubic polynomial airfoil

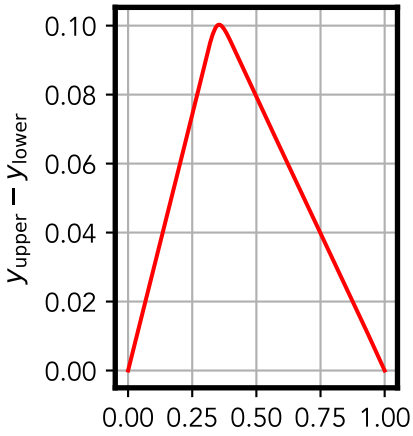


c) Thickness profile of optimal cubic polynomial airfoil

**Fig. 2 Minimum supersonic drag cubic airfoil subject to various constraints, cubic spline.**

We ran this problem using both a cubic spline representation of the airfoil, with $n = 40$, and a cubic polynomial representation. The results of the cubic spline solution are shown in Fig. 2 and the results of the cubic polynomial solution are shown in Fig. 3. A superimposed comparison of the resulting airfoils is shown in Fig. 4. The spline case demonstrated a 28.75% reduction in drag ($c_d = 0.058$ vs $c_d = 0.082$).

The physical airfoil generated in the spline case is intuitively similar to the classic test case of the diamond airfoil as the minimum drag airfoil in an unconstrained supersonic thin airfoil problem. However, in this case the center point of

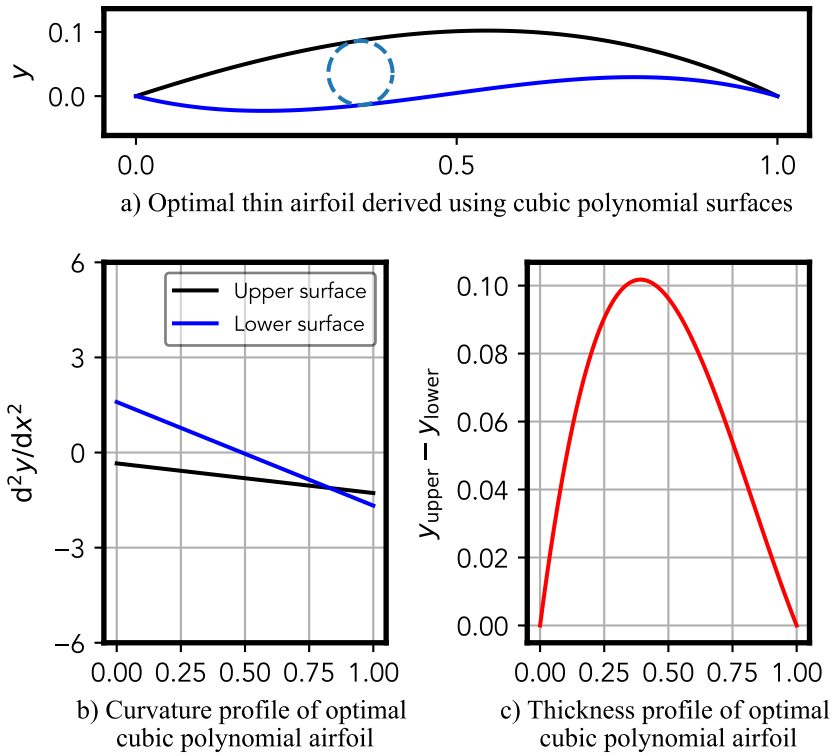


**Fig. 3 Minimum supersonic drag cubic airfoil subject to various constraints, cubic polynomial.**

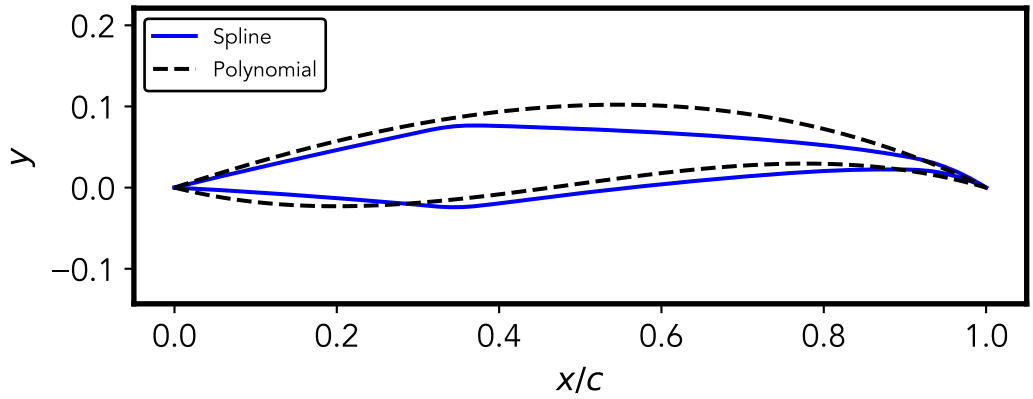


**Fig. 4 Minimum supersonic drag cubic airfoil subject to various constraints, cubic polynomial compared to cubic spline.**

the diamond has been shifted to accommodate the prescribed internal payload and the trailing edge has been sculpted to meet the subsonic maximum angle of zero lift and maximum moment coefficient constraints.

### C. Sensitivity Analysis

The solution of the previous section raises several issues related to the use of these, more flexible, splines. First, each new segment introduces six additional constraints as well as two additional quadratic forms into the objective function. In the interest of computational efficiency it would be helpful to understand how many knots are appropriate in order to reap increased airfoil performance using this additional flexibility without introducing unnecessary computational complexity into the problem. Second, the traditional diamond airfoil does not account for other important effects in the significant portion of flight time that any aircraft will spend in the subsonic flight regime. For the previous problems, the maximum absolute curvature in the spline case is nearly twice that of the polynomial case. These zones of high curvature are potential areas of boundary layer separation and ensuing poor aerodynamic performance. Therefore, it would be helpful to understand the relative tradeoff between drag improvement and variation in curvature. In this section we will explore both of these important dynamics.

#### *1. Regularization Parameter*

The design of physical surfaces generally favors so-called *fair* surfacing[17], whereby the surface will not demonstrate significant waves, or stated more simply, curvature should vary relatively smoothly.

In order to minimize this variation of curvature, we add a small of regularization to the sum of the third derivative (or the derivative of curvature) to the objective function. By varying the regularization constant for this term, we can generate a family of optimal airfoil shapes that will provide an understanding of the tradeoff between allowable curvature variation and potential drag reduction over the polynomial case.

$$\underset{v,y_c}{\text{minimize}} \qquad \frac{4}{\lambda\sqrt{M^2-1}}\sum_i v_i^T Q_i v_i + \frac{\lambda}{2n}\sum_i \left(a_{u_i}^2 + a_{l_i}^2\right) \tag{34}$$

For the example shown above, the value of this additional term, without multiplier, $\lambda$, is approximately 80, whereas, $c_d = 0.058$, approximately a three order of magnitude difference. Fig. 5 shows the tradeoff of varying the $\lambda$ parameter, both in the resulting drag coefficient as well as the maximum forebody curvature ($x \leq 0.75c$) vs drag coefficient. Similarly, Fig. 6 shows the physical effect on airfoil shape of varying this parameter. Larger values provide a smoother surface, while smaller values allow for sharper edges with higher curvature.

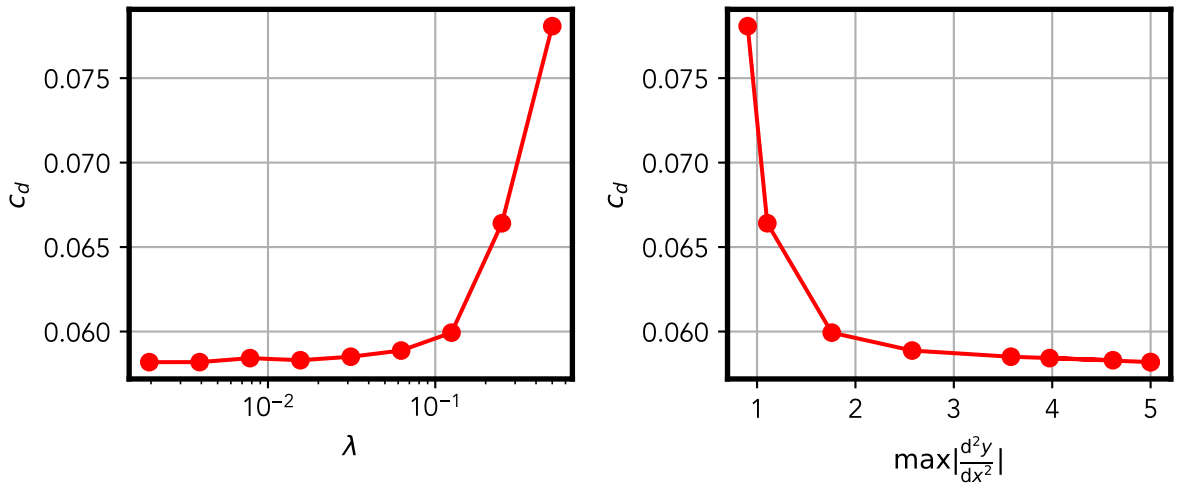


**Fig. 5 Drag coefficient as function of $\lambda$, $n = 40$.**

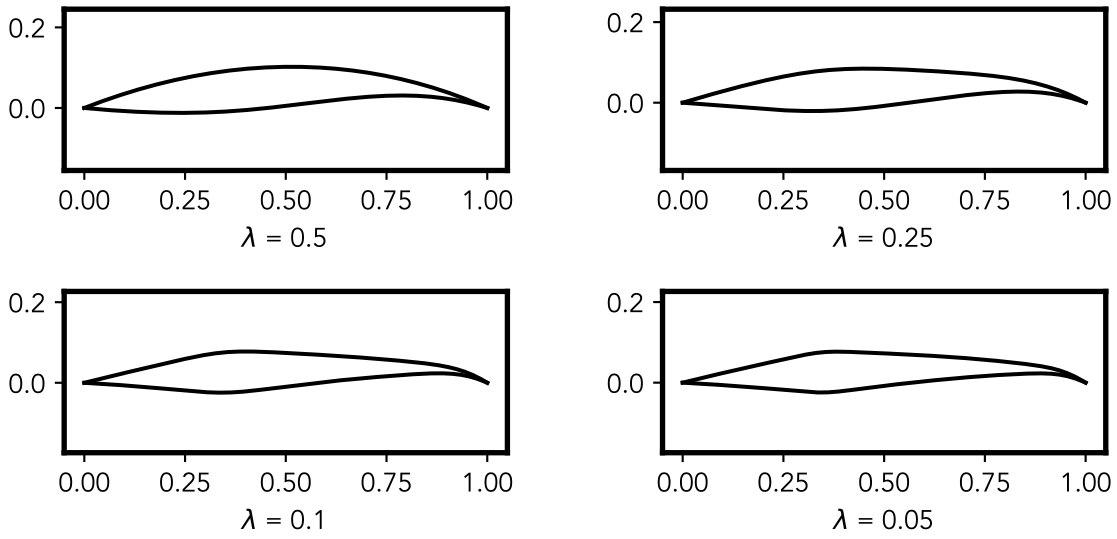


**Fig. 6 Optimal drag airfoils for varying $\lambda$, $n = 40$.**

*2. Length of Knot Vector*

The number of knots, or polynomial segments, is also a critical input to the optimization problem in the case of cubic splines. Too few segments will not give the optimizer the flexibility to find a truly optimal solution, too many will result in unnecessary computational expense. In this section we will attempt to understand the appropriate number of knots to include in this class of problem. Below, we shown two cases of calculated optimal drag, the first in Fig. 7 with $\lambda = 0.25$, and the second, in Fig. 8, with a regularization term of $\lambda = 0.001$. As seen in each, for this problem, the error converges in the vicinity of 40 knots, which seems an appropriate general guideline.

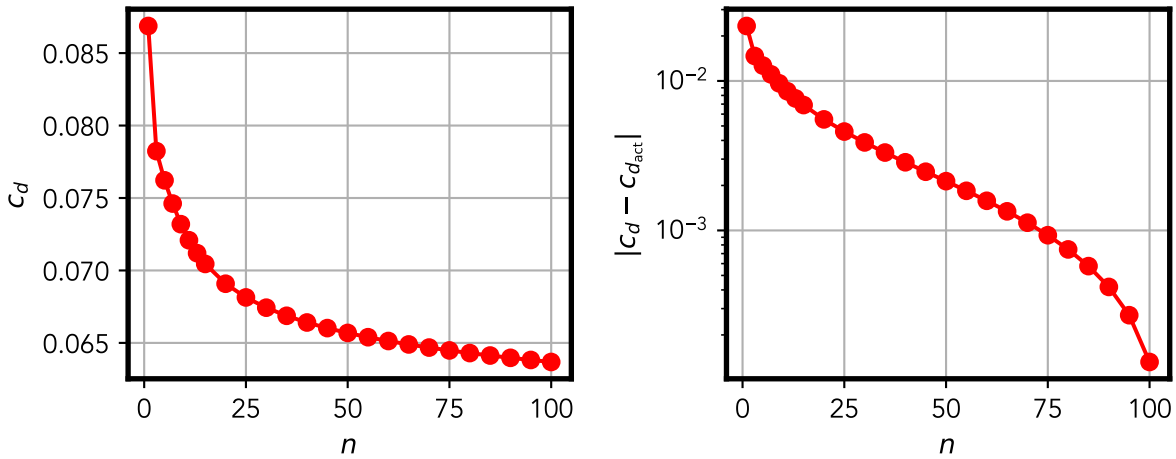


a) Calculated drag coefficient b) Drag coefficient error

**Fig. 7 Error in drag coefficient with increasing knots, $\lambda = 0.25$.**

**D. Minimum Drag Supersonic Airfoil with Variable Internal Payload**

Here we refine our previous results by choosing the number of spline knots and the regularization parameter using the result of the previous section. Additionally, we employ bisection to solve a nonconvex extension, with an internal

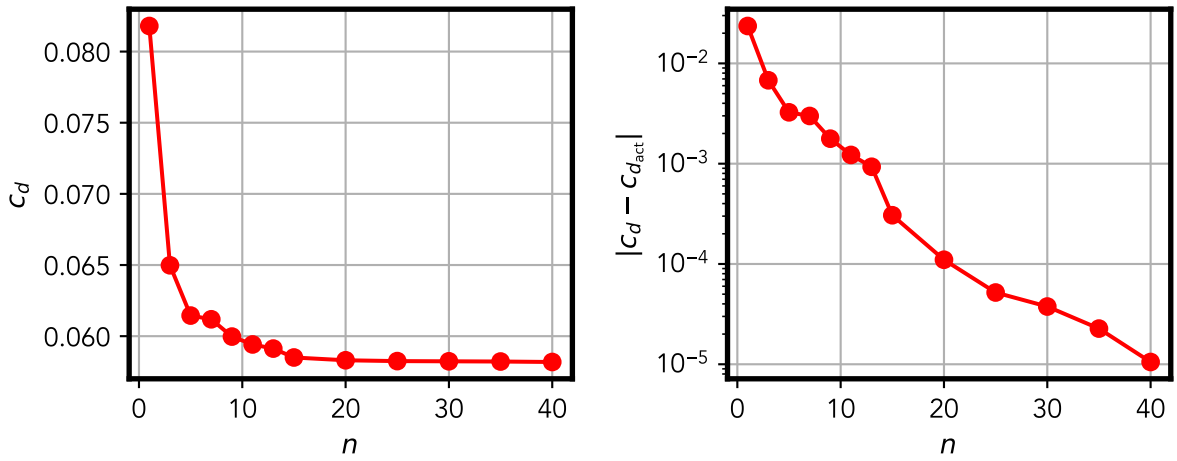


a) Calculated drag coefficient b) Drag coefficient error

**Fig. 8 Error in drag coefficient with increasing knots, $\lambda = 0.001$.**

payload where the location, $x_c$ is now variable, but the spline coefficient design vector, $v$ is the same as before,

$$
\begin{aligned}
\underset{v,y_c,x_c}{\text{minimize}} \quad & \frac{4}{\lambda\sqrt{M^2-1}} \sum_i v_i^T Q_i v_i + \frac{\lambda}{2n} \sum_i \left(a_{u_i}^2 + a_{l_i}^2\right) \\
\text{subject to} \quad & \alpha_{l0} \le \alpha_{l0_{\min}} \\
& c_{\text{mac}} \le c_{\text{mac}_{\max}} \\
& \alpha = 0 \\
& \min_{x\in[0,1]} \; (y_u(x) - y_l(x)) \ge 0 \\
& \max_{x\in[0,1]} \; |y_u''(x) - y_l''(x)| \le \kappa_{\max} \\
& \min_{\theta\in[0,\pi]} \left(a_{u_i}(x_c + r\cos\theta)^3 + b_{u_i}(x_c + r\cos\theta)^2 + c_{u_i}(x_c + r\cos\theta) + d_{u_i} - y_c - r\sin\theta\right) \ge 0 \\
& \max_{\theta\in[\pi,2\pi]} \left(a_{l_i}(x_c + r\cos\theta)^3 + b_{l_i}(x_c + r\cos\theta)^2 + c_{l_i}(x_c + r\cos\theta) + d_{l_i} - y_c - r\sin\theta\right) \le 0.
\end{aligned}
\tag{35}
$$

We solve this problem using a golden-section search, which includes two solutions of the inner convex problem, with $x_c$ fixed, per iteration. Fig. 9 shows the interval width ($|b - a|$) at each interval and convergence history.

For values of $M = 2$, $n = 40$, $\lambda = 0.25$, $r = 0.05$, $\alpha_{l0_{\min}} = -0.15$, $c_{\text{mac}_{\max}} = -0.2$, and $\kappa_{\max} = 5$, we obtain the following results. The optimal drag coefficient, $c_d = 0.064$. The optimal placement of the internal payload is $x_c = 0.485$ and $y_c = 0.037$. The angle of attack for zero lift, $\alpha_{l0} = -0.150$ and the moment coefficient about he aerodynamic center, $c_{\text{mac}} = -0.264$. Fig. 10 shows the resulting airfoil shape, curvature, and thickness profile. Again demonstrating an airfoil cross section influenced by the optimal diamond shape, for minimal supersonic drag in a small disturbance field, with higher camber near the trailing edge to meet the subsonic lift and moment constraints and a modest amount of curvature across the airfoil to prevent subsonic flow separation. Furthermore, the use of cubic splines decreases the optimal drag by approximately 20.15% as compared with the polynomial case ($c_d = 0.080$), with the comparitive shapes shown in Fig. 11.

## V. Conclusion

In this paper, we have extended an approach to conceptual airfoil design, in circumstances where the assumptions of thin-airfoil theory hold, that provides a global optimum in polynomial time using convex optimization techniques. These techniques provide the designer with a ready menu of options for objective function and constraints that allow for the application of a variety of aerodynamic and geometric constraints. We have provided derivations for relevant objective functions and constraints for shapes represented by cubic splines and have shown an approximately 20%

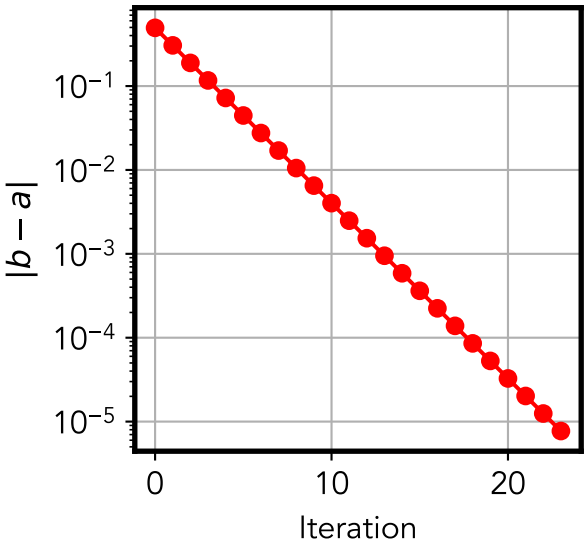


**Fig. 9 Residual history of nonconvex, golden-section search.**

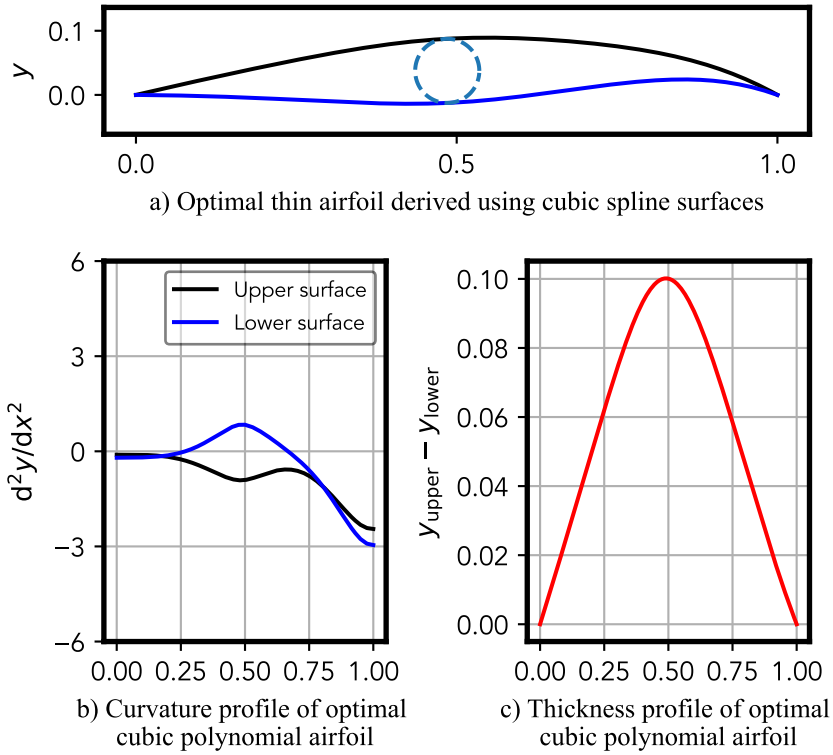


**Fig. 10 Optimal results derived from golden-section search,** $\lambda = 0.25$**.**

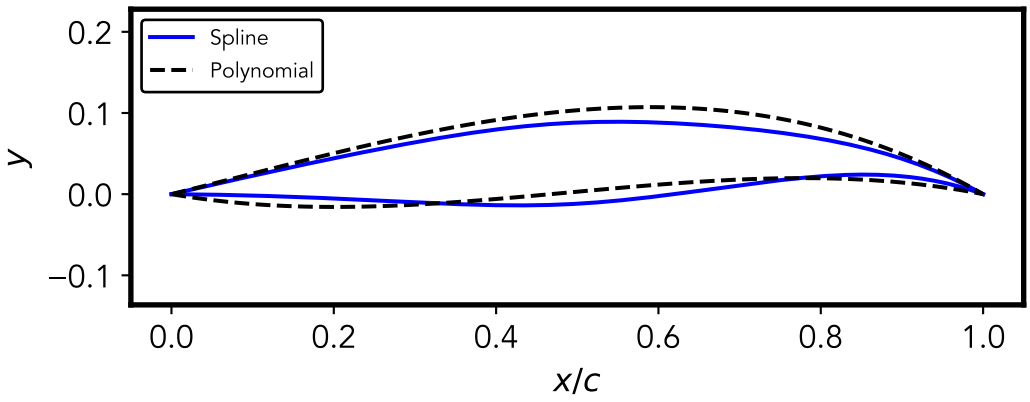


**Fig. 11 Comparison of resulting cubic polynomial and cubic spline airfoils.**

decrease in drag coefficient by providing the optimizer with this increased flexibility. Finally, we have shown the impact of several important problem parameters in the quality of the final solution, and applied these concepts to a nonconvex extension of the initial supersonic drag minimization problem.

## References


[1] Berkenstock, D., Alonso, J., and Lessard, L., "A Convex Optimization Approach to Thin Airfoil Design," *AIAA Aviation Forum*, 2022.

[2] Boyd, S., and Vandenberghe, L., *Convex Optimization*, Cambridge University Press, 2004.

[3] Song, W., and Keane, A., "A Study of Shape Parameterisation Methods for Airfoil Optimisation," *10th AIAA/ISSMO Multidisciplinary Analysis and Optimization Conference*, 2012.

[4] Masters, D. A., Taylor, N. J., Rendall, T., Allen, C. B., and Poole, D. J., "Review of Aerofoil Parameterisation Methods for Aerodynamic Shape Optimisation," *53rd AIAA Aerospace Sciences Meeting*, 2015.

[5] Sripawadkul, V., Padulo, M., and Guenov, M., "A Comparison of Airfoil Shape Parameterization Techniques for Early Design Optimization," *13th AIAA/ISSMO Multidisciplinary Analysis Optimization Conference*, 2012.

[6] Kulfan, B., and Bussoletti, J., ""Fundamental" Parameteric Geometry Representations for Aircraft Component Shapes," *11th AIAA/ISSMO Multidisciplinary Analysis and Optimization Conference*, 2006.

[7] Kulfan, B. M., "Universal Parametric Geometry Representation Method," *Journal of Aircraft*, Vol. 45, 2008, pp. 142–158.

[8] Kulfan, B., "A Universal Parametric Geometry Representation Method - "CST"," *45th AIAA Aerospace Sciences Meeting and Exhibit*, 2007.

[9] Rajnarayan, D., Ning, A., and Mehr, J. A., "Universal Airfoil Parametrization Using B-Splines," *2018 Applied Aerodynamics Conference*, 2018.

[10] Li, W., and Krist, S., "Spline-Based Airfoil Curvature Smoothing and Its Applications," 2005, pp. 1065–1074.

[11] Beach, R., *An Introduction to the Curves and Surfaces of Computer-aided Design*, Van Nostrand Reinhold, 1991.

[12] Moran, J., *An Introduction to Theoretical and Computational Aerodynamics*, Dover Books on Aeronautical Engineering, Dover Publications, 2013.

[13] Kuethe, A. M., and Chow, C., *Foundations of aerodynamics: Bases of aerodynamic design*, 3rd ed., Wiley New York, 1976.

[14] Diamond, S., and Boyd, S., "CVXPY: A Python-embedded modeling language for convex optimization," *Journal of Machine Learning Research*, Vol. 17, No. 83, 2016, pp. 1–5.

[15] Agrawal, A., Verschueren, R., Diamond, S., and Boyd, S., "A rewriting system for convex optimization problems," *Journal of Control and Decision*, Vol. 5, No. 1, 2018, pp. 42–60.

[16] Löfberg, J., "YALMIP: A toolbox for modeling and optimization in MATLAB," *IEEE International Conference on Robotics and Automation*, 2004, pp. 284–289.

[17] Botsch, M., Kobbelt, L., Pauly, M., Alliez, P., and Levy, B., *Polygon Mesh Processing*, CRC Press, 2010.